Allometric scaling of thermal infrared emitted from UK cities and its relation to urban form City and Environment Interactions

Abdulrasheed, Mukhtar; MacKenzie, A. Robert; Whyatt, Duncan; Chapman, Lee

DOI:
10.1016/j.cacint.2020.100037

Document Version
Publisher's PDF, also known as Version of record

Citation for published version (Harvard):
Abdulrasheed, M, MacKenzie, AR, Whyatt, D & Chapman, L 2020, 'Allometric scaling of thermal infrared emitted from UK cities and its relation to urban form City and Environment Interactions', *City and Environment Interactions*, vol. 5, 100037. https://doi.org/10.1016/j.cacint.2020.100037

City and Environment Interactions 5 (2020) 100037

Contents lists available at ScienceDirect

City and Environment Interactions

journal homepage: www.elsevier.com/locate/cacint

Allometric scaling of thermal infrared emitted from UK cities and its relation to urban form

M. Abdulrasheed [a], A.R. MacKenzie [a,b,*], J.D. Whyatt [c], L. Chapman [a]

[a] School of Geography, Earth and Environmental Science, University of Birmingham, Edgbaston, B15 2TT Birmingham, UK
[b] Birmingham Institute of Forest Research, University of Birmingham, Edgbaston, B15 2TT Birmingham, UK
[c] Lancaster Environment Centre, Lancaster University, Lancaster LA1 4YQ, UK

ARTICLE INFO

Article history:
Received 25 February 2020
Received in revised form 27 May 2020
Accepted 30 May 2020
Available online 3 June 2020

Keywords:
Urban Heat Island (UHI)
Land Surface Temperature (LST)
Allometry
Urban size and population
Geographic information system (GIS)
MODIS and emitted energy

ABSTRACT

As a result of differences in heat absorption and release between urban and rural landscapes, cities develop a climate different from their surroundings. The rise in global average surface temperature and high rates of urbanization, make it important to understand the energy balance of cities, including whether any energy-balance-related patterns emerge as a function of city size. In this study, images from the Moderate Resolution Imaging Spectro-radiometer (MODIS) satellite instrument, covering the period between 2000 and 2017, were sampled to examine the seasonal (winter and summer) night-time clear-sky upwelling long-wave energy for 35 UK cities. Total (area-summed) emitted energy per overpass per city is shown to correlate closely ($R^2 \geq 0.79$) with population on a log-log 'allometry' plot. The production of emitted energy from the larger cities is smaller than would be produced from a constellation of smaller cities housing the same population. The mean allometry slope over all overpasses sampled is 0.84 ± 0.06, implying an 'economy (or parsimony) of scale' (i.e., a less-than-proportional increase) of about 21% (i.e. $100(2–10^{0.84\log(2)})$) for each doubling of city population. City area shows a very similar economy of scale, so that the scaling of night-time emitted energy with urban area is close to linear (1.0 ± 0.05). This linearity with area indicates that the urban forms used in UK cities to accommodate people more efficiently per unit area as the urban population grows, do not have a large effect on the thermal output per unit area in each city. Although often appearing superficially very different, UK cities appear to be similar in terms of the components of urban form that dictate thermal properties. The difference between the scaling of the heat source and literature reports of the scaling of urban-rural air (or surface) temperature difference is very marked, suggesting that the other factors affecting the temperature difference act to decrease strongly its scaling with population.

1. Introduction

Urbanization is accelerating across the world, especially in developing countries across Africa and Asia [1,2]. Current projections indicate that by 2050, the global urban population will increase by 2.4 billion, i.e., about half the current population of 4.22 billion (United Nation 2019) [3–6]. The change of land surface characteristics caused by urbanization leads, amongst other things, to changes in the local energy balance that must be taken into account when determining long-term temperature trends [7]. This change in thermal climate in urban areas, leads to the urban heat island (UHI), which is the tendency of an urban area to have warmer near-surface air temperatures than its rural surroundings [8–11,128,130]. Related phenomena include: urban thermal plumes [10,12] and urban precipitation anomalies [13].

Recent conceptual UHI models have emphasised the importance of different land uses within cities [14,15], highlighting the prospect that urban planning choices can be used to mitigate adverse urban climate trends [16,17]. Implicit in most studies of UHI, from Howard [18] on, is that local, one-dimensional (i.e., vertical), energy budgets for urban land uses, combine through the action of fluid stirring and mixing, to produce a three-dimensional dome of urban heating over a city — see, for example, the very widely reproduced cross-sections of UHI through an idealised city (e.g., [19]).

We hypothesise that gross changes in urban form affect the storage of solar heating as the size of cities increase. We focus on night-time, clear-sky, emitted long-wave energy as a primary measure of heat storage, and we use population as our measure of city size. We use an extensive property — total emitted energy (in Megawatts) per city per night — rather than intensive property such as temperature or emission per unit area, to permit direct comparisons with other extensive properties such as urban area, and to explore the extent to which the behaviour of intensive properties, particularly UHI, differ from the behaviour of the extensive properties.

* Corresponding author at: School of Geography, Earth and Environmental Science, University of Birmingham, Edgbaston, B15 2TT Birmingham, UK.
E-mail address: a.r.mackenzie@bham.ac.uk. (A.R. MacKenzie).

http://dx.doi.org/10.1016/j.cacint.2020.100037

1.1. Urban form and urban heat

The urban form of a city is the result of its social, economic, and environmental context. We focus on UK cities in this study; further work will focus on a different setting in order to try and distinguish the general from that dependent on UK context [20]. A recognised system of UK urban planning mostly originates from the industrial revolution, prior to which most people lived and worked in the countryside [21,22]. As industries grew, people migrated to towns and cities in search of better wages, opportunities, and livelihoods [23] leading to rapid growth in town and cities. Many decrees and ordinances were issued to manage this growth, including, at the beginning of the 20th century, the Town Planning Act 1909, which was introduced to ensure that local authorities prepared schemes of town planning. This was followed by the Housing Act 1919, which required the design of houses to be approved by the Ministry of Health, and the Housing Act 1930, which required clearance of high-density 'slums', which were considered unsanitary [24]. The post-war 1940s was a period of uncertainty for the architects and town planners tasked with rebuilding Britain's bomb-damaged cities [25–27]. Residential rebuilding in this period often involved the replacement of low-rise private dwellings with fewer, but larger, high-rise public buildings [24], sometimes with an intermediate period of low-rise prefabricated structures [28]. Cities across the UK such as Bristol, Coventry, Hull, Portsmouth, Southampton and Plymouth were very severely damaged during World War II [29], and so were subject to significant post-war changes. For those neighbourhoods, which, by the 1960s and 1970s, had escaped slum clearance or destruction in wartime, the tendency was for renewal rather than replacement of low-rise and mid-rise residential buildings [24]. In the subsequent decades, and until the present day, a more laissez-faire approach has dominated, with renewal and replacement of housing and commercial buildings through private-public cost sharing of various kinds [24,29,30].

Emerging in parallel, from the latter part of the nineteenth century and through the first part of the 20th century, was the Garden Cities movement, which advocated public health improvement by planning to build cities with more, and more accessible, green spaces, see e.g., [31]. This advocacy eventually led to the New Towns movement and New Towns Act 1946 [32–35] which resulted in towns such as Telford, Letchworth and Milton Keynes. All the 20th-century housing and town planning policies in the UK led to notable changes in the urban form from the scale of individual dwellings, through neighbourhood scale land-use, to the patterns of use across whole urban areas.

The nature and patterns of urban form (i.e. building geometry, pervious surface fraction, building and tree densities, soil permeability etc.) determine the thermal characteristics of place. Such characteristics can be used to define local climate zones (LCZ) [36], which may vary over time as a result of planned or unplanned changes. For example, slum clearance often re-shaped low-rise, close-packed, terraced housing into a sparse array of high-rise towers e.g., [24]. Suburban extension of cities replaced farm field (or, often, filled in parkland estates around large houses) with semi-detached two storey housing in wide boulevards (shifting from linear form to cul-de-sac mid-century). Infilling (building in what had previously been back gardens) became prominent towards the end of the 20th century [37].

As cities grow, green space — trees and vegetation — are replaced with grey space, i.e., buildings and transport and utility infrastructure. The magnitude and nature of the change is often sporadic and patchy, and results in a wide variety of urban forms [38,39]. In terms of the surface energy balance, changing from rural to urban land results, in general, in the absorption of a higher fraction of incoming solar radiation and a decrease in the Bowen ratio (i.e., the ratio of sensible to latent heat emission) [40,41]. Energy absorption and emission at the ground surface is therefore a key driver of urban climate, strongly influencing the near surface air temperature and the radiant fluxes relevant for health effects (e.g., [42,43]). Satellite based studies report thermal emission as land-surface temperature (or 'skin' temperature), from which surface UHI intensity (SUHII) can be derived (e.g., [44–46,123,128,129]). In-situ sensing reports air temperature directly. Near-surface air temperature UHI and SUHII do not always correspond for a variety of physical reasons [11,41,47–49] but both are driven by absorption and emission of energy at the ground surface. The fundamental role of surface energy exchange motivates us to investigate how surface energy parameters vary for a set of cities of very different size and urban form, in order to understand this foundational driver of both the UHI and SUHII.

Buildings also slow the wind near the surface, retaining the heat released from vehicles and buildings [50,51]. Energy removed from the mean wind is lost to the surfaces or transformed into turbulent kinetic energy, affecting the dissipation of scalars such as temperature and trace-gas pollutants e.g., [52]. Dense building arrangements decrease the sky-view factor [53–55]. The net result of all these changes is the increased storage of heat, which is the root cause of the UHI effect. Increased heat storage can lead to a number of issues such as human health risk [42,43,56–62], environmental hazard (e.g., [63]), and infrastructure failure [64,65], which themselves add heat to urban air and often require further energy consumption to offset [66].

Researchers have long studied the effects of urban form on climate change, and the impacts of climate change on urban environment, as reviewed in [67,68]. Urban planning responses to urban heat and climate change, including both mitigation and adaptation strategies, continue to evolve, especially with respect to sustainable urban development in cities [69–74]. Urban climate adaptation focuses on reducing vulnerability and promoting resilience of people and properties [75–77]. Microclimate planning and design modification to outdoor environment can also enhance thermal comfort, e.g., neighbourhood streets trees, green spaces and parks, [78,79]. We expect that planning responses to urban heat will manifest in the relationship of urban form to city size.

1.2. Allometry and urban heat

Allometry is originally a concept from biology, relating morphological and physiological aspects of organism biology to some more easily measured parameters such as body mass [80–83]. Allometric approaches were introduced to urban studies (e.g. [84–86]) and used to model the relationship between a set of cities and the largest city within a geographical region [83]. Urban allometry studies have sought to elucidate decadal evolution of urbanized area [81,87], fractal spatial patterning [88], income inequality [89], and between urban form and growth [90]. Interpretations drawn from urban allometry include growth by innovation driven by economies of scale [91], and urban form as a hierarchy of clusters, [92].

In general, for urban studies, allometric scaling relates aspects of urban material, energy, or economic flows to the size of cities as determined by their population [81,91–93,125–127]. Because it focuses on the relative rate of change of properties with size, referred to as 'scaling' below, allometry lends itself to comparative studies of properties of very different character [94]. In our previous study of air pollutant emissions and concentrations, we found it informative to compare the scaling of an intensive property (urban air concentrations) with the scaling of extensive properties (area-summed pollutant emissions and urban area) [95].

Allometric scaling recognises that the many microscopic interactions within a complex system often collapse to a simple pattern [96,127]. Scaling, therefore, allows us a synthesising perspective on cities [91], by searching for simple patterns without becoming overwhelmed by details of local context.

Allometric patterns, where they exist, conform closely to an equation of the form:

$$Y = \beta X^{\alpha} \tag{1a}$$

The power law, Eq. (1a), describes a straight-line relationship between the X and Y variables when the function is plotted on a double logarithmic coordinate system, i.e.

$$log(Y) = log(\beta) + \alpha.\ log(X) \tag{1b}$$

where $log(\beta)$ is a constant offset and α is the rate of relative growth (the allometric scaling factor or, simply, slope). Below, we will refer to α as defining the 'scaling' of Y with respect to X.

Using allometry, this study seeks a quantitative scaling relationship between population and clear-sky upwelling emitted energy, in order to determine whether and how the many detailed processes affecting this part of the urban energy budget combine at the city-scale. The study evaluates whether simplicity emerges from urban complexity with respect to emitted long-wave. We compare our findings on clear-sky upwelling long-wave to a classical result in the literature of urban heat islands.

The empirical relationship between the UHI and structure of a city arises from the fact that tall, close-packed, concrete and brick buildings store solar energy in day time and emit it at night more slowly than a flat surface [97]. The thermal infrared energy emitted from a surface is acted on by wind and radiation transfer processes; structural elements of a city affecting wind and radiative transfer will therefore influence UHI [98]. Since structural elements of cities are often laid out block by block, one approach to analysing a city is to determine its energy budget and surface temperature explicitly on a block-by-block basis [99,100]. Land-use categories and urban morphology types offer useful approaches to determining modifications to the surface energy budget that will produce a nocturnal urban heat Island [9,101,102]. Other urban climate studies focus on the effect of the urban surface at the neighbourhood scale, using land-use classifications to generalise results (e.g. [14,41]). At city scale the number of studies are fewer: [9] for North American settlements; [103] for Korea; [104] for Kansas City; and [105] for Montreal and Vancouver.

Several studies in the urban climate literature offer an allometric perspective [106–108], and many other comparative studies show that UHI or SUHII increases with some measure of the size of the city (e.g. [45,109,124]) or focus on the largest cities because the UHI is assumed to be largest there (e.g., [44,46]). Oke [98,107] presented the relationship between a measure of maximum UHI ($\Delta T_{u\text{-}r}$(max)) and population for European settlements (Fig. 1) and supports the hypothesis that the canopy air temperature, $\Delta T_{u\text{-}r}$, is a function of city size, with the absolute UHI increasing by about 0.6 °C (i.e. $1.975.\log_{10}(2)$) for every doubling in population. Zhou et al. [109] fitted a sigmoidal curve to the log-linear relationship of SUHII to urban area. The sigmoidal function is approximately linear for urban clusters with areas between 2 and 200 km^2 with SUHII increasing by ~0.3 °C for an area doubling (Zhou et al., their Fig. 2). Zhou et al. [45] plot SUHII against $\log_e$(urban area) similarly to find a log-linear regression in which SUHII increases by about 0.4 °C (i.e. $0.55.\log_e(2)$) for an area doubling.

Fig. S1 in the Supplementary Information presents the Oke [98] data in a power-law log-log graph. Regressing on $\log_{10}(\Delta T_{u\text{-}r}(max))$ gives more weight to the smaller cities, but a strong relationship is still found. The scaling of $\Delta T_{u\text{-}r}$ in Fig. S1 is small, 0.11 ± 0.03, but significantly different from zero — and equivalent to an increase of just 8% (i.e. $100(10^{0.11.\log(2)}\text{-}1)$) in UHI for a population doubling. Using a similar log-log regression, Manoli et al. [106] found a scaling with population of $\log_{10}$(SUHII) ranging between 0.15 and 0.24, equivalent to a maximum increase of 18% (i.e. $100(10^{0.24.\log(2)}\text{-}1)$) for a population doubling. Such relatively modest scalings with population have implications, such as that 'densification' of population into large urban centres presents a rather modest increased contribution of air temperature to thermal discomfort and associated health risk, at least to the extent that this can be gauged by the UHI of the 20th century city forms in Oke's [98,107] sample.

Having identified the best-fit scaling relationship, the residual offset from this best-fit for any individual city is also informative [112]. The residual for any city on any night, $r_{j,k}$, is calculated as the vertical distance of the datum for that city to the best-fit line:

$$r_{j,k} = \log(Y_{j,k}) - \{ log(\beta_k) + \alpha_k . log(X_j) \} \quad (2)$$

where $Y_{j,k}$ is the measured value of dependent variable (in our case, the summed emitted energy of city, j, on a given night, k), X_j is the population, of city j, and the parameters α_k and β_k define the allometric scaling relationship. In Oke's scaling data (Figs. 1 and S1), the largest-magnitude residual is a large negative deviation (i.e. less heat island than expected) for the UK town of Reading [98].

Since both the canopy air temperature UHI, and the surface temperature SUHII result from heat storage, the scaling of emitted energy (with population or urban area) will be an important contributor to the scaling of UHI and SUHII. When the observed scaling of emitted energy is larger than that for UHI or SUHII, other factors must be acting to dampen the overall scaling. Thus, this paper seeks to use allometric scaling, and importantly an interpretation of the residual offset, to inform the role of bulk urban morphology as a control for levels of urban heat.

2. Methodology

2.1. The study area

According to the Office for National Statistics (ONS), the population of UK as at 30th June 2016 is estimated to be 65,648,000, concentrated in urban areas in the southern half of the country (Fig. 2a), and with a rate of increase of 0.8% (538,000) per annum [113]. The climate of UK is temperate, but variable, particularly because of altitude and distance from the coast (Fig. 2b). Average temperature is 4 °C January (winter) and 15 °C in July (summer) [114,115]. Mean climate data are shown in Fig. 2. This study focuses on thirty-five (35) large (area > 50 km^2) settlements in the Great British mainland of the UK (see Fig. 2a below and table S1 and fig. S5 in supplementary section SI). Boundaries for the cities were extracted from medium scale digital map data (Meridian2; see Data Sources, below) produced by the Ordnance Survey (GB National Mapping Agency) and

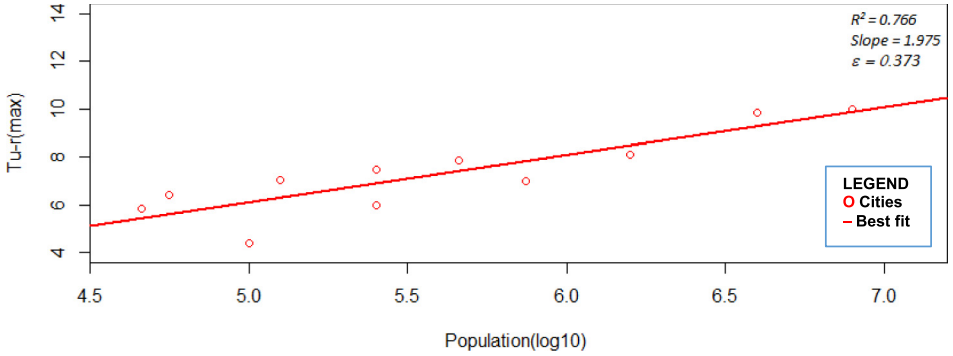

Fig. 1. Relation between maximum air temperature heat island intensity ($\Delta T_{u\text{-}r}$ (max), degrees Celsius) and population (P) for European Settlements (redrawn from [107]). Sources of $\Delta T_{u\text{-}r}$ (max) are literature and private communications dating from 1927 to 1972. It is not clear in Oke [98,107] if the population data used is matched in time to the date for $\Delta T_{u\text{-}r}$ (max). Reported on the graph (top right) are the Coefficient of Determination (R^2) for the best-fit regression, the slope of the regression, and the error on the slope (ε).

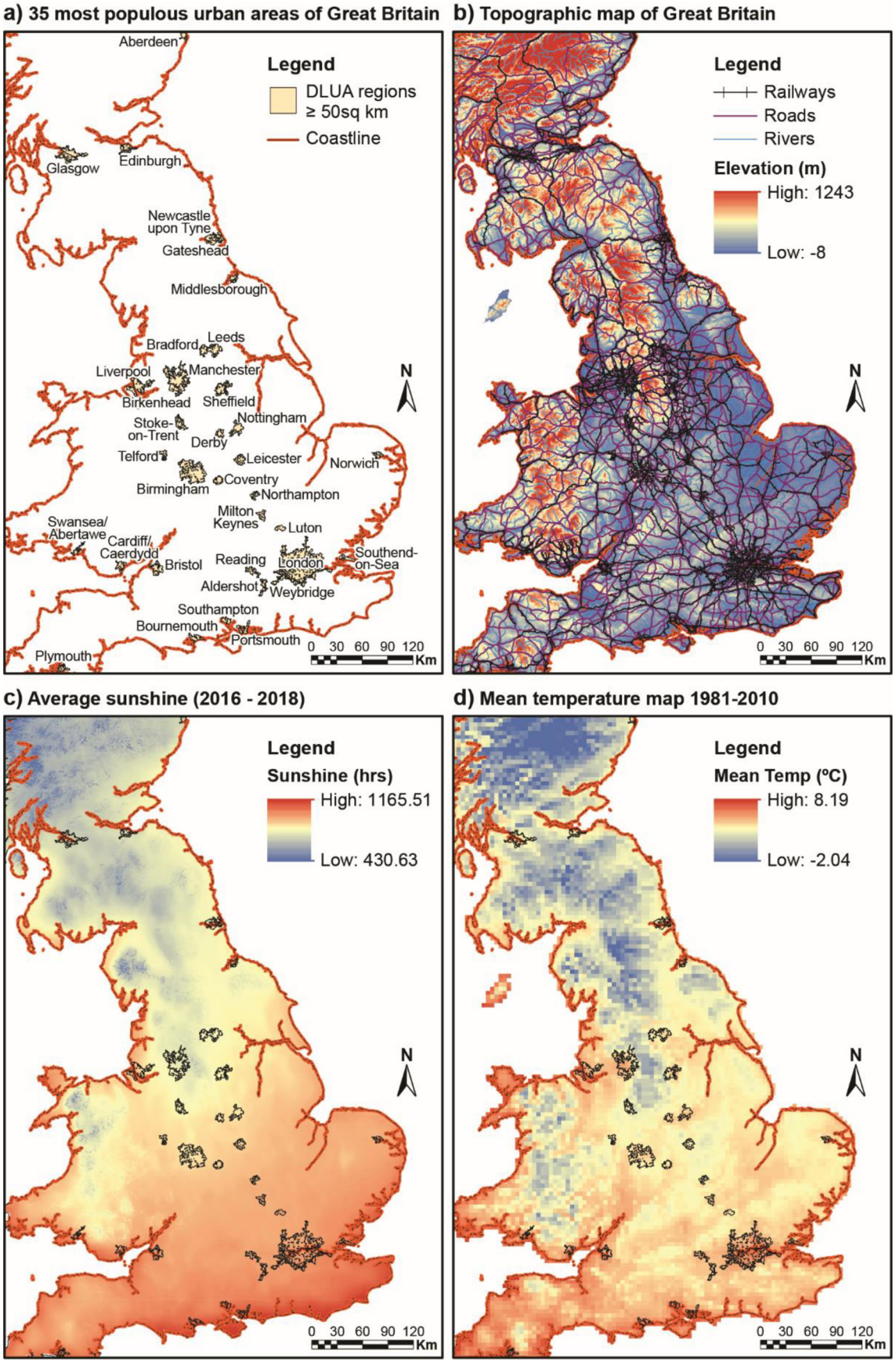

Fig. 2. (a) 35 most populous urban areas in Great Britain (urban boundaries are contiguous Developed Land Use Areas from Meridian2 data); (b) Topographic map of central Great Britain with cities and major roads; (c) Average Sunshine of central Great Britain; (d) Mean 2 m Temperature map of central Great Britain. The data were sourced from Centre for Environmental Data Analysis [110,111], and ArcGIS tool were used to plot the maps.

represent contiguous Developed Land Use Areas (DLUA) rather than administrative demarcations. UHI, SUHII, and urban allometry studies are sensitive to the choice of urban boundary and this should be borne in mind in the comparisons discussed below. The urban boundary used to define population in Oke [98] is likely administrative; the urban cluster areas used in Zhou et al. [45,109] are similar to our contiguous DLUA. Population counts were retrieved from the Office of National Statistics [113] at the lowest level of geographical aggregation (output area) and attributed to the contiguous DLUAs.

2.2. Data collection and analysis

This study uses MODIS/Terra V006 composite products (MOD11A1) – MODIS/Terra Land Surface Temperature and Emissivity Daily L3 Global 1 km Grid SIN V006 [116]. This product provides gridded, high resolution, cloud-cleared, quality-controlled and quality-assured data, and has accurate calibration in multiple thermal infrared bands designed for retrievals of Land Surface Temperature (LST) and atmospheric properties [116,117]. LST from MODIS are retrieved from clear sky observations at daytime and night-time with the aid of a generalized split-window algorithm [117,118]. It is established that satellite sensors looking in the nadir can oversample horizontal urban surfaces and undersample vertical surfaces [41,48]. This will tend to overemphasise both day-time heating and night-time cooling, the extent of which varies with the angle of view. Angle of view also affects the native spatial resolution of the satellite radiances; interpolation in the MOD11A1 processing pipeline brings the dataset to a uniform 1-km grid. The MOD11A1 dataset contains information on view angle but we have not implemented any further correction for off-nadir view geometries. For simplicity, only night-time overpasses (0130 h local time) are considered for the present study.

Area-summed clear-sky night-time long-wave upwelling emitted energy (hereafter 'emitted energy') for mainland Great Britain was derived for selected days from 2000 to 2017. We interpret emitted energy in preference to LST because it gives proper weighting to radiance from the highest temperatures and provides a sum in physically meaningful units. The LST data used was selected to have as much clear sky over the region as possible. LST data for each pixel, i, within the city, j, on night, k, was converted to emitted energy, $\epsilon_{i,j}$ in W m^{-2}, using the Boltzmann law:

$$\epsilon_{i,j,k} = \sigma T_{i,j,k}^4 \tag{3}$$

where, σ is the Stefan-Boltzmann constant = 5.67 × 10^{-8} W m^{-2} K^{-4}, and $T_{i,j,k}$ is the LST in Kelvin. The effect of varying surface emissivity is not taken into account. Area-summed emitted energy, $<E_j>$ in MW, for each city on each night, was then calculated by summing the p unobscured land-surface pixels inside the city boundary:

$$\langle E_{j,k} \rangle = \Sigma_{i=0}^{p} \epsilon_{i,j,k} \;\; a \tag{4}$$

where $\Delta a = 1$ km^2 and the factor of 10^6 converting km^2 into m^2 is accommodated in the units of $<E_j>$. A default 50% threshold of clear sky was set for each city on each image based on the assumption that adequate coverage of the study region can be achieved by sampling a large enough set of imagery. The threshold was implemented in ArcGIS simply by comparing the maximum area of each city as given by the Meridian dataset (Table S1) with the area inside the city containing valid LST (i.e. p.Δa) from the satellite dataset. The effect of using a 75% clear-sky threshold is discussed below.

2.3. Scaling study methodology

35 cities were selected for study using an arbitrary threshold of city area greater than 50 km^2, from which population and emitted energy were derived (table S3 in SI). Clear-sky nights were selected based on the prevalent synoptic meteorology (i.e., fog-free anticyclone conditions in the absence of fronts). A total of 28 nights was selected: 15 in winter (30 November – 28 February) and 13 in summer (1 June − 31 August) in the period 2000 — 2017.

3. Results

Area-summed emitted energy varies over 1.5 orders of magnitude for cities with populations ranging over 2 orders of magnitude (Fig. 3a). Although the exact slope varies from night to night (Fig. 3b), the tight log-log correlation is always present. Strong correlations are present on both summer and winter nights (Table 1) with no obvious pattern, suggesting that scaling of emitted energy may not be as seasonal as the UHI or SUHII itself (cf. [109,119,129]). The correlations suggest that population is a good predictor variable for total emitted energy, despite substantial differences in urban form of British cities. Fig. 3b shows the plots for all dates sampled in this study. Slopes are similar, varying between 0.73 ± 0.06 (13 December 2010; Table 1) and 0.92 ± 0.09 (17 December 2011) and are ranked in Table 1 by their R^2 value when using a 50% cloud-free threshold. Standard error on the slope increases as R^2 decreases but there is no obvious trend in the value of the slope.

The derived regression equation for the averaged allometry over 28 nights is:

$$\log(\overline{Y}) = \log(\overline{\beta}) + \overline{\alpha}.\, \log\left(\overline{\langle E_j \rangle}\right), \tag{5}$$

where

$$\overline{\langle E_j \rangle} = \frac{\Sigma_{k=0}^{n} E_{j,k}}{n}. \tag{6}$$

That is, $\overline{\langle E_j \rangle}$ is the average emitted energy (in MW) over all nights for city, j, and n is the number of nights = 28.

Although the two extreme values of the allometric slope are statistically different (i.e., the means are further apart than the sum of the standard errors, Table S3, Supplementary SI), Fig. 3a does not show any clustering of the regression slopes in the sample. It is assumed, therefore, that, to a first approximation at least, the results indicate that a single overall allometric scaling of total emitted energy with population of 0.84 ± 0.06 is plausible (Fig. 3b). If this assumption is justified, the variation observed in the regression slope must derive from difficult-to-quantify errors in the retrieval of the emitted energies, including the effect of partially obscured urban areas on the slope.

To test the impact of partial cloud obscuring, the analysis was repeated increasing the threshold for inclusion of an urban area in the analysis to 75% cloud-free (see Table S3 and Fig. S6 in supplementary SI). The scaling of emitted energy with population under this more stringent condition has a slope of 0.86 ± 0.05 (Table S3 in Supplementary SI), which is, within error, indistinguishable from the mean slope from Table 1.

Table S4 (supplementary SI) tests the effect of a population threshold by comparing the correlations for cities with populations >250,000 and >500,000. The mean slope of the regression is not significantly different for both subsets of cities.

4. Discussion

The findings from this study indicate that population is a good predictor variable for total emitted energy despite the differences in the urban form of UK cities. This study finds a much more significant scaling for upwelling clear-sky long-wave with population than was found for $\Delta T_{u\text{-}r}$ (max) by Oke [98,107] (i.e., Fig. S1 in SI). Energy emitted from the surface is acted on by turbulent and radiative transfer processes, the net result of which is $\Delta T_{u\text{-}r}$ (max) [107]. Although it is plausible that turbulent transfer processes scale with city size (as discussed in [95]), it appears that the overall effect on the energy budget is to dampen very significantly the scaling of $\Delta T_{u\text{-}r}$ (*max*) compared to the scaling of emitted energy. The difference in the scalings of the heat source and the final temperature difference is very marked. Investigating this further will require a detailed investigation of the scaling

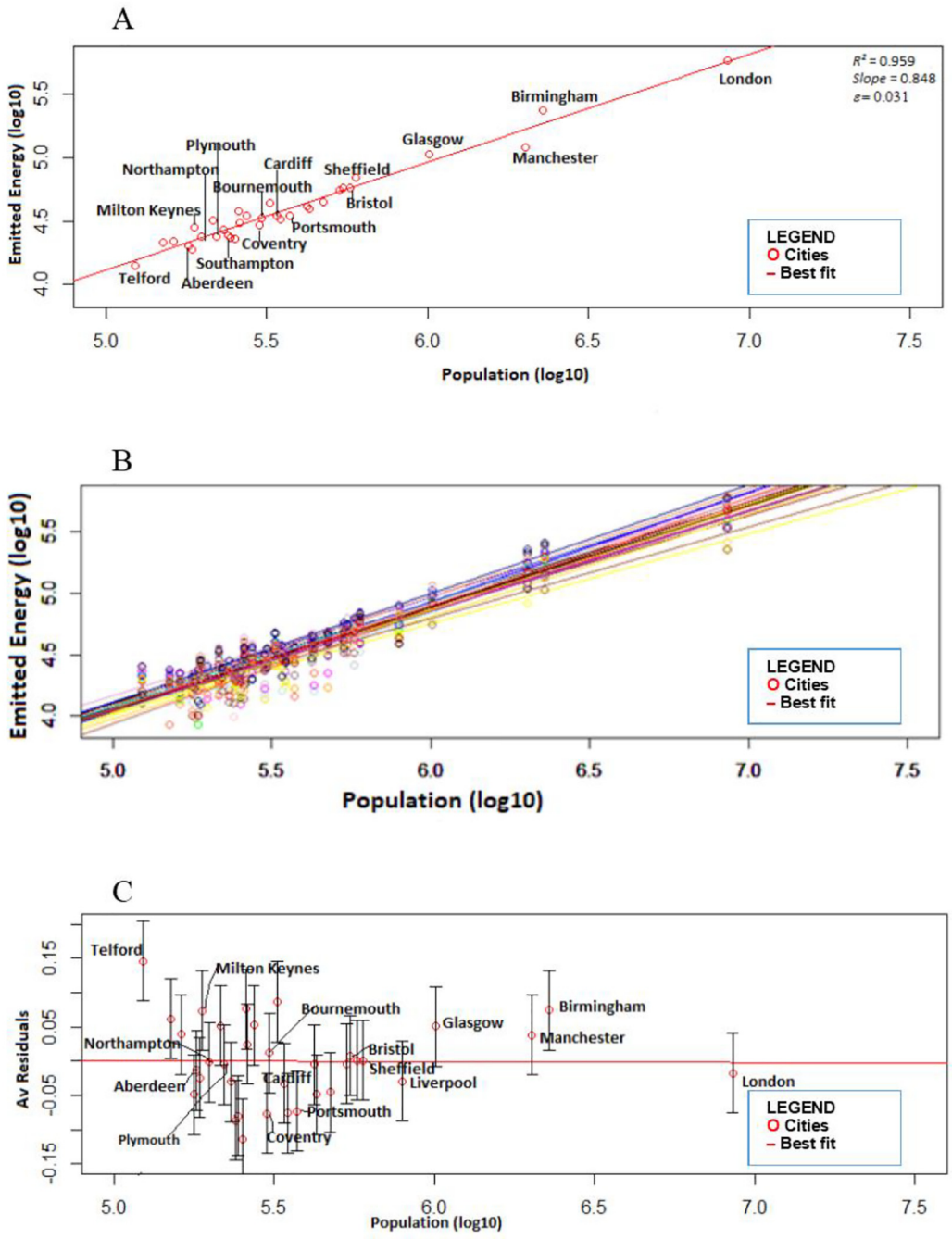

Fig. 3. (A) An example of allometric scaling of night-time emitted energy $Log_{10}(<E_j>$, in MW) against urban population for the 35 largest cities in Great Britain. Reported on the graph (top right) are the Coefficient of Determination (R^2) for the best-fit regression, the slope of the regression, and the error on the slope (ε). (B) The ensemble of allometric relationships derived for the nights studied (Table 1). (C) Residual emitted energy (mean and standard deviation of $Log_{10}(<E_j>$ in MW) for urban areas with respect to the allometric scalings shown in (B).

of each aspect of the urban energy budget, which is outside the scope of the present study.

The scaling of emitted energy with population is very similar to that of total urban area with population (Fig. S2A in the SI). Hence, emitted energy varies linearly with urban area for the 35 cities in our study (Fig. S3), even though that area becomes increasingly densely populated as city population increases. The implication is that, on average, there is no structural change of relevance to the total emitted energy between a single city the size of London or ten cities each a tenth of the area (i.e., roughly the size of Bristol). This quantitative scaling without qualitative structural change may be consistent with [98] study on city size and the urban heat Island, and with his study in 1981 on canyon geometry and the nocturnal urban heat Island, in which he cited Chandler's 1967 observation on the similarities of London and Leicester temperature on the same night, despite their difference in size and population [98,102]. Non-linearities may become more important when smaller urban centres are included, as in the study of Zhou et al. [109].

Further information pertaining to the urban form can be derived by inspection of the residuals, i.e., the distances of each urban area from the line of best fit (Fig. 3c). We postulate that differences in urban form across Great British cities will be evident in both the magnitude and sign of the residuals. Firstly, however, we discount geographical and climate factors. Comparisons between mean emitted-energy residuals and each of altitude, latitude, mean hours of sunshine, and mean annual temperature for each city

Table 1
Night-time emitted energy for thirty-five (35) UK large Cities on selected summer and winter nights. Results are ranked by the strength (R^2) of the log-log correlation between emitted energy and population, for which the slope, and error on slope are reported at 50% cloud free pixels.

Rank	Date	Number of cities	R^2	Slope (α)	Error on slope
1	13th Feb. 2017	26	0.97	0.86	0.03
2	15th Feb. 2016	25	0.96	0.85	0.03
3	06th Jun. 2000	33	0.96	0.85	0.03
4	22nd Feb. 2003	28	0.96	0.88	0.04
5	07th Jul. 2007	34	0.96	0.84	0.03
6	01st Jan. 2007	32	0.96	0.85	0.03
7	02nd Jan. 2017	35	0.94	0.84	0.04
8	26th Dec. 2009	24	0.93	0.81	0.05
9	27th Jun. 2010	32	0.93	0.80	0.04
10	16th Aug. 2016	35	0.92	0.89	0.04
11	29th Feb. 2000	21	0.92	0.83	0.05
12	01st Jan. 2012	24	0.92	0.89	0.06
13	30th Nov. 2016	20	0.92	0.86	0.06
14	13th Dec. 2010	17	0.92	0.73	0.06
15	28th Aug. 2001	25	0.91	0.88	0.06
16	30th Aug. 2005	22	0.90	0.82	0.06
17	20th Jan. 2009	18	0.88	0.83	0.08
18	09th Jul. 2006	34	0.88	0.88	0.06
19	20th Jan. 2011	22	0.88	0.74	0.06
20	08th Aug. 2012	25	0.88	0.83	0.06
21	05th Jan. 2005	34	0.88	0.80	0.05
22	10th Jun. 2003	27	0.87	0.81	0.06
23	13th Jul. 2002	28	0.87	0.77	0.06
24	03rd Aug. 2017	22	0.86	0.82	0.07
25	25th Feb. 2009	26	0.85	0.91	0.08
26	28th Aug. 2009	30	0.84	0.81	0.07
27	17th Dec. 2011	26	0.83	0.92	0.09
28	18th Feb. 2006	25	0.79	0.84	0.09
	Mean			0.84	0.06
	Median			0.83	

showed no significant correlations (see Figs. S9, S10, S11 and S12 in supplementary SI).

The magnitude of residual can be interpreted as the degree to which an individual city deviates positively or negatively from the value expected for a city of its size [112]. For the case of emitted thermal energy, positive anomalies correspond to cities with warmer surfaces than expected and negative anomalies correspond to surfaces cooler than expected based on the best-fit population-based allometry. There is a tendency for the magnitude of residuals to be larger for the smaller urban areas (Fig. 3c). For example, the residual for Telford is positive and about 4% of its mean area-summed emission, whereas, for London, the residual is about 0.2% of the mean area-summed emission.

The cities of Coventry and Plymouth, which were reconstructed post-war [29] have large negative residuals (-0.075 and -0.004 y-axis units ($\log_{10}(<E_j>$ in MW)), Fig. 3c), whereas the New Town 'Garden Cities' of Milton Keynes and Telford both have large positive residuals (0.08 and 0.15 units). These unexpected results do not seem to arise from sampling issues affecting the overall allometry because the residuals are robust for the various nights studied (variation bars in Fig. 3c). Instead, the results may arise from a greater area of impervious, low albedo, surface per person in the lower density Garden Cities. Residuals for the area allometry for each city are reported in (table S2 supplementary SI). Milton Keynes and Telford have large positive residuals compared to their expected area (0.087 and 0.155 units, respectively), whilst Coventry and Plymouth have large negative residuals (-0.056 and -0.050 units). So, the Garden cities emit more than expected for their populations but spread that emission over a wider surface area than expected, whereas Coventry and Plymouth emit much less than expected from their population but spread that emission over a smaller-than-expected area.

Northampton, situated about 60 miles (97 km) north-west of London and 45 miles (72 km) south-east of Birmingham, had a population of 212,100 at the 2011 census. Northampton is predominantly a post-war settlement in which growth was limited until it was nominated as a New Town in 1968 [120]. Its mean energy emission residual is close to zero, similar to Bristol (Fig. 3c), despite being radically different in terms of population and their histories of urban development. The residuals for urban area are also similar for Northampton and Bristol. However, Milton Keynes, the city closest to Northampton in population (Table 1, supplementary SI), similarly situated (about 50 miles (80 km) north-west of London), and also a classic post-war New Town, has a large positive mean emitted energy residual (Fig. 3c) and large positive area residual.

City configuration, street patterns and orientation, structure of buildings and density, and ultimately the intensity of human activities are key factors that determine thermal behaviour in the city. In summary, the residuals (Fig. 3c) allow an assessment of the similarities and differences in emitted energy, relative to that expected by the best-fit line, for settlements of very different size.

5. Conclusion

This study aimed at evaluating the extent and rate of clear-sky emitted long-wave energy with population in the cities for MODIS/Terra V006 composite products (MOD11 A1). This was achieved by assessing the night-time emitted energy across cities in Great Britain for 28 night-time samples across summer and winter between 2000 and 2017. British cities show a strong and consistent sub-linear allometric scaling of total emitted energy with population. That is, there is a substantial 'economy (or parsimony) of scale' in terms of nocturnal heat production in British cities: the production from the larger cities is smaller than would be produced from a constellation of smaller cities housing the same population. This uniformity of scaling occurs despite of the obvious differences in architecture and urban form in settlements with Medieval centres (e.g. Aberdeen), predominantly commercial/military (e.g. Southampton) or residential (Bournemouth) coastal settlements, and post-second-world-war planned settlements (e.g., Milton Keynes).

The scaling of emitted energy with population is much larger than the scaling reported in the literature for the scaling of air temperature urban heat island (UHI) with population [98,107] or for the scaling of surface urban heat island intensity (SUHII) [45,109]. It is possible to compare these scalings even though emitted energy and UHI or SUHII have different units, because the logarithmic scaling produces a dimensionless slope quantifying relative changes (e.g., [94]). Since long-wave emissions from the relatively warm urban surface are the source of the nocturnal UHI and SUHII, turbulent and radiative transfer in the atmosphere must act to dampen significantly the scaling signal for heat island metrics. The concentration of population into larger urban areas, rather than spread out over more, smaller, cities, has only a marginal worsening effect on the risk to health arising from air temperature UHI but a much larger effect arising from radiant flux (cf., e.g., [43]).

The scaling of total emitted energy with population has a similar slope, within statistical error, as the scaling of urban area with population. This equality of scaling suggests that energy emitted per unit area averages out to be approximately the same everywhere in cities at the granularity of the current analysis. This 'emergent simplicity' in the scaling of emitted energy for urban areas of different sizes seems counter intuitive given our understanding of the role of urban form in heat storage and emission in the built environment [121,122]. Instead, the particularities of British urban form seem to manifest in the residuals for each city, i.e., the magnitude of the difference in emitted energy measured from that predicted by the best-fit line. As yet, we have not been able to find any simple rules that would allow us to predict the size of the residual from its geographical context (including climate) or from its development history but we believe this merits further study.

CRediT authorship contribution statement

M. Abdulrasheed: Investigation, Writing - original draft. **A.R. MacKenzie:** Conceptualization, Supervision, Writing - review & editing. **J.D. Whyatt:** Investigation, Writing - review & editing. **L. Chapman:**

Conceptualization, developed from earlier work by JDW and ARMK, Supervision, Writing - review & editing.

Acknowledgements

We very gratefully acknowledge the substantial work of the referees and editor to improve the manuscript. ARMK and LC acknowledge support from the WM Air project of the Natural Environment Research Council (NE/S003487/1). MA gratefully acknowledges support from the Petroleum Technology Development Fund.

Appendix A. Supplementary data

Supplementary data to this article can be found online at https://doi.org/10.1016/j.cacint.2020.100037.

References

[1] Cohen B. Urbanization in developing countries: current trends, future projections, and key challenges for sustainability. Technol. Soc. Sustainable Cities. 2006;28:63–80. https://doi.org/10.1016/j.techsoc.2005.10.005.
[2] Martins PB. Urbanizing world [WWW document]. URL; 2000. http://www.prb.org/Publications/Reports/2000/AnUrbanizingWorldPDF619KB.aspx. [Accessed 26 November 2017].
[3] Bongaarts J. Human population growth and the demographic transition. Philos Trans R Soc B Biol Sci. 2009;364:2985–90. https://doi.org/10.1098/rstb.2009.0137.
[4] Bremner J, Frost A, Haub C, Mather M, Ringheim K, Zuehlke E. World population highlights: key findings from PRB's 2010 world population data sheet. Popul Bull. 2010;65:1–12.
[5] Buhaug H, Urdal H. An urbanization bomb? Population growth and social disorder in cities Glob Environ Change. 2013;23:1–10. https://doi.org/10.1016/j.gloenvcha.2012.10.016.
[6] Seto KC, Güneralp B, Hutyra LR. Global forecasts of urban expansion to 2030 and direct impacts on biodiversity and carbon pools. Proc Natl Acad Sci. 2012;109:16083–8. https://doi.org/10.1073/pnas.1211658109.
[7] Chrysanthou A, van der Schrier G, van den Besselaar EJM, Klein Tank AMG, Brandsma T. The effects of urbanization on the rise of the European temperature since 1960. Geophys Res Lett. 2014;41:7716–22. https://doi.org/10.1002/2014GL061154.
[8] Bornstein RD. Observations of the urban heat island effect in New York City. J Appl Meteorol. 1968;7:575–82. https://doi.org/10.1175/1520-0450(1968)007<0575:OOTUHI>2.0.CO;2.
[9] Landsberg HE. The urban climate. Academic Press; 1981.
[10] Oke TR. The Heat Island of the urban boundary layer: characteristics, causes and effects, in: wind climate in cities. Dordrecht: NATO ASI Series. Springer; 1995;81–107. https://doi.org/10.1007/978-94-017-3686-2_5.
[11] Sheng L, Tang X, You H, Gu Q, Hu H. Comparison of the urban heat island intensity quantified by using air temperature and Landsat land surface temperature in Hangzhou. China Ecol Indic. 2017;72:738–46. https://doi.org/10.1016/j.ecolind.2016.09.009.
[12] Heaviside C, Cai X-M, Vardoulakis S. The effects of horizontal advection on the urban heat island in Birmingham and the West Midlands, United Kingdom during a heatwave. Q J Roy Meteorol Soc. 2015;141:1429–41. https://doi.org/10.1002/qj.2452.
[13] Han J-Y, Baik J-J, Lee H. Urban impacts on precipitation. Asia-Pac J Atmospheric Sci. 2013;50. https://doi.org/10.1007/s13143-014-0016-7.
[14] Stewart ID, Oke TR. Local climate zones for urban temperature studies. Bull Am Meteorol Soc. 2012;93:1879–900. https://doi.org/10.1175/BAMS-D-11-00019.1.
[15] Tomlinson CJ, Chapman L, Thornes JE, Baker CJ. Derivation of Birmingham's summer surface urban heat island from MODIS satellite images. Int J Climatol. 2012;32:214–24. https://doi.org/10.1002/joc.2261.
[16] Davoudi S. Climate change, securitisation of nature, and resilient urbanism. Environ Plan C Gov Policy. 2014;32:360–75. https://doi.org/10.1068/c12269.
[17] Davoudi S. Climate risk and security: new meanings of "the environment" in the English planning system. Eur Plan Stud. 2012;20:49–69. https://doi.org/10.1080/09654313.2011.638491.
[18] Howard L. The climate of London, Vol. 1; 1818 London.
[19] Lemmen DS, Warren FJ, editors. Climate change impacts and adaptation: a Canadian perspective. Natural Resources Canada: Climate Change Impacts and Adaptation Program; 2004 Available from: . https://cfs.nrcan.gc.ca/publications?id=27428.
[20] Abdulrasheed M. The effect of spatial settlement patterns on urban climatology. PhD Thesis Birmingham, UK: University of Birmingham; 2020.
[21] CPRE. Campaign to protect rural England|38 degrees [WWW document]. URL. https://you.38degrees.org.uk/partnerships/campaign-to-protect-rural-england; 2018. [Accessed 28 September 2019].
[22] Inikori JE. A historiography of the first industrial revolution [WWW document]. Afr Ind Revolut Engl Study Int Trade Econ Dev. 2002. https://doi.org/10.1017/CBO9780511583940.004.
[23] Karp M. A very old book: the case for Eric Hobsbawm's age of revolution. URL: The Junto; 2013. https://earlyamericanists.com/2013/02/07/a-very-old-book-the-case-for-eric-hobsbawms-age-of-revolution/. [Accessed 29 December 2018].
[24] Carmon N. Three generations of urban renewal policies: analysis and policy implications. Geoforum. 1999;30:145–58. https://doi.org/10.1016/S0016-7185(99)00012-3.
[25] Ball M, Maginn PJ. Urban change and conflict: evaluating the role of partnerships in urban regeneration in the UK. Hous Stud. 2005;20:9–28. https://doi.org/10.1080/0267303042000308705.
[26] Hollow M. Utopian urges: visions for reconstruction in Britain, 1940–1950. Plan Perspect. 2012;27:569–85. https://doi.org/10.1080/02665433.2012.705126.
[27] Tsubaki T. Planners and the public: British popular opinion on housing during the second world war. Contemp Br Hist. 2000;14:81–98. https://doi.org/10.1080/13619460008581573.
[28] Short JR. Housing in Britain: the post-war experience. Routledge, London. New: York; 1982.
[29] Hasegawa J. The attitudes of the Ministry of Town and Country Planning towards blitzed cities in 1940s Britain. Plan Perspect. 2013;28:271–89. https://doi.org/10.1080/02665433.2013.737712.
[30] Webb MS. Local responses to the protection of medieval buildings and archaeology in British post-war town reconstruction: Southampton and Coventry. Urban Hist. 2018;45:635–59. https://doi.org/10.1017/S0963926818000019.
[31] Burnett J. Social history of housing by Burnett - AbeBooks [WWW document]. https://www.abebooks.co.uk/book-search/title/social-history-of-housing/author/burnett/; 1986. [Accessed 29 September 2019].
[32] Alexander A. Britain's new towns: Garden cities to sustainable communities. Routledge; 2009.
[33] Goist PD. Patrick Geddes and the city. J Am Inst Plann. 1974;40:31–7. https://doi.org/10.1080/01944367408977444.
[34] Rubin NH. The changing appreciation of Patrick Geddes: a case study in planning history. Plan Perspect. 2009;24:349–66. https://doi.org/10.1080/02665430902933986.
[35] Tizot J-Y. Ebenezer Howard's Garden City Idea and the Ideology of Industrialism Cah Victoriens Edouardiens. 2018:87. https://doi.org/10.4000/cve.3605.
[36] Stewart ID, Oke TR, Krayenhoff ES. Evaluation of the 'local climate zone' scheme using temperature observations and model simulations. Int J Climatol. 2014;34:1062–80. https://doi.org/10.1002/joc.3746.
[37] Whitehand JWR, Whitehand SM. The study of physical change in town centres: research procedures and types of change. Trans Inst Br Geogr. 1983;8:483–507. https://doi.org/10.2307/621964.
[38] Hopkins MIW. The ecological significance of urban fringe belts. Urban Morphol. 2012;16:41–54.
[39] Morris AEJ. History of urban form, geo. London: Godwin; 1974.
[40] Aguado E, Burt JE. Understanding weather and climate [WWW document]. https://www.pearson.com/us/higher-education/product/Aguado-Understanding-Weather-and-Climate-7th-Edition/9780321987303.html; 2015. [Accessed 17 December 2018].
[41] Arnfield AJ. Two decades of urban climate research: a review of turbulence, exchanges of energy and water, and the urban heat island. Int J Climatol. 2003;23:1–26. https://doi.org/10.1002/joc.859.
[42] Basu R, Samet JM. Relation between elevated ambient temperature and mortality: a review of the epidemiologic evidence. Epidemiol Rev. 2002;24:190–202. https://doi.org/10.1093/epirev/mxf007.
[43] Middel A, Krayenhoff ES. Micrometeorological determinants of pedestrian thermal exposure during record-breaking heat in Tempe, Arizona: introducing the MaRTy observational platform. Sci Total Environ. 2019;687:137–51. https://www.sciencedirect.com/science/article/pii/S0048969719326531.
[44] Peng S, Piao S, Ciais P, Friedlingstein P, Ottle C, Bréon F-M, et al. Surface urban Heat Island across 419 global big cities. Environ Sci Technol. 2012;46:696–703. https://doi.org/10.1021/es2030438.
[45] Zhou B, Rybski D, Kropp JP. The role of city size and urban form in the surface urban heat island. Sci Rep. 2017;7:1–9. https://doi.org/10.1038/s41598-017-04242-2.
[46] Zhou D, Zhao S, Liu S, Zhang L, Zhu C. Surface urban heat island in China's 32 major cities: spatial patterns and drivers. Remote Sens Environ. 2014;152:51–61. https://doi.org/10.1016/j.rse.2014.05.017.
[47] Schwarz N, Lautenbach S, Seppelt R. Exploring indicators for quantifying surface urban heat islands of European cities with MODIS land surface temperatures. Remote Sens Environ. 2011;115:3175–86. https://doi.org/10.1016/j.rse.2011.07.003.
[48] Voogt JA, Oke TR. Effects of urban surface geometry on remotely-sensed surface temperature. Int J Remote Sensing. 1998;19(5):895–920.
[49] Voogt JA, Oke TR. Thermal remote sensing of urban climates. Remote Sens Environ. 2003;86(3):370–84.
[50] Arifwidodo SD, Tanaka T. The characteristics of urban Heat Island in Bangkok, Thailand. Procedia - soc. behav. sci., world conference on technology. Innovation and Entrepreneurship. 2015;195:423–8. https://doi.org/10.1016/j.sbspro.2015.06.484.
[51] Golden JS. The built environment induced urban heat island effect in rapidly urbanizing arid regions – a sustainable urban engineering complexity. Environ Sci. 2004;1:321–49. https://doi.org/10.1080/15693430412331291698.
[52] Belcher SE, Jerram N, Hunt JCR. Adjustment of a turbulent boundary layer to a canopy of roughness elements. J Fluid Mech. 2003;488:369–98. https://doi.org/10.1017/S0022112003005019.
[53] Chapman L, Thornes JE. Real-time sky-view factor calculation and approximation. J Atmos Oceanic Tech. 2004;21(5) [WWW Document]. URL . https://journals.ametsoc.org/doi/full/10.1175/1520-0426%282004%29021%3C0730%3ARSFCAA%3E2.0.CO%3B2. [Accessed 21 August 2019].
[54] Grimmond S. Urbanization and global environmental change: local effects of urban warming. Geogr J. 2007;173:83–8. https://doi.org/10.1111/j.1475-4959.2007.232_3.x.
[55] Yang J, Wong MS, Menenti M, Nichol J. Modeling the effective emissivity of the urban canopy using sky view factor. ISPRS J Photogramm Remote Sens. 2015;105:211–9. https://doi.org/10.1016/j.isprsjprs.2015.04.006.

[56] Hondula DM, Balling RC, Vanos JK, Georgescu M. Rising temperatures, human health, and the role of adaptation. Curr Clim Change Rep. 2015;1:144–54. https://doi.org/10.1007/s40641-015-0016-4.

[57] Krayenhoff ES, Moustaoui M, Broadbent AM, Gupta V, Georgescu M. Diurnal interaction between urban expansion, climate change and adaptation in US cities. Nat Clim Change. 2018;8:1097. https://doi.org/10.1038/s41558-018-0320-9.

[58] Murray V, Ebi KL. IPCC special report on managing the risks of extreme events and disasters to advance climate change adaptation (SREX). J Epidemiol Community Health. 2012;66:759–60. https://doi.org/10.1136/jech-2012-201045.

[59] Patz JA, Campbell-Lendrum D, Holloway T, Foley JA. Impact of regional climate change on human health. Nature. 2005;438:310–7. https://doi.org/10.1038/nature04188.

[60] Rosenzweig C, Solecki WD, Hammer SA, Mehrotra S. Climate change and cities: First assessment report of the urban climate change research network. Cambridge University Press; 2011.

[61] Smith CL, Webb A, Levermore GJ, Lindley SJ, Beswick K. Fine-scale spatial temperature patterns across a UK conurbation. Clim Change. 2011;109:269–86. https://doi.org/10.1007/s10584-011-0021-0.

[62] Wouters H, De Ridder K, Poelmans L, Willems P, Brouwers J, Hosseinzadehtalaei P, et al. Heat stress increase under climate change twice as large in cities as in rural areas: a study for a densely populated midlatitude maritime region. Geophys Res Lett. 2017;44:8997–9007. https://doi.org/10.1002/2017GL074889.

[63] Chapman L, Thornes JE. A geomatics-based road surface temperature prediction model. Sci. Total Environ., Urban Environmental Research in the UK: The Urban Regeneration and the Environment (NERC URGENT) Programme and associated studies. 2006;360:68–80. https://doi.org/10.1016/j.scitotenv.2005.08.025.

[64] Chapman L, Bell SJ. High-resolution monitoring of weather impacts on infrastructure networks using the internet of things. Bull Am Meteorol Soc. 2018;99:1147–54. https://doi.org/10.1175/BAMS-D-17-0214.1.

[65] Dawson RJ, Thompson D, Johns D, Wood R, Darch G, Chapman L, et al. A systems framework for national assessment of climate risks to infrastructure. Philos Transact A Math Phys Eng Sci. 2018;376. https://doi.org/10.1098/rsta.2017.0298.

[66] Li M, Shi J, Guo J, Cao J, Niu J, Xiong M. Climate impacts on extreme energy consumption of different types of buildings. PLoS One. 2015;10:e0124413. https://doi.org/10.1371/journal.pone.0124413.

[67] Mills G. Cities as agents of global change. Int J Climatol. 2007;27:1849–57. https://doi.org/10.1002/joc.1604.

[68] Seto KC, Sánchez-Rodríguez R, Fragkias M. The new geography of contemporary urbanization and the environment. Annu Rev Env Resour. 2010;35:167–94. https://doi.org/10.1146/annurev-environ-100809-125336.

[69] Castán Broto V. Urban governance and the politics of climate change. World Dev. 2017;93:1–15. https://doi.org/10.1016/j.worlddev.2016.12.031.

[70] Davoudi S, Crawford J, Mehmood A. Planning for climate change: strategies for mitigation and adaptation for spatial planners; 2009 [Earthscan].

[71] Fujii H, Iwata K, Managi S. How do urban characteristics affect climate change mitigation policies? J Clean Prod. 2017;168:271–8. https://doi.org/10.1016/j.jclepro.2017.08.221.

[72] Hendrickson TP, Nikolic M, Rakas J. Selecting climate change mitigation strategies in urban areas through life cycle perspectives. J Clean Prod. 2016;135:1129–37. https://doi.org/10.1016/j.jclepro.2016.06.075.

[73] Jabareen YR. Sustainable urban forms: their typologies, models, and concepts. J Plan Educ Res. 2006;26:38–52. https://doi.org/10.1177/0739456X05285119.

[74] Rybski D, Reusser DE, Winz A-L, Fichtner C, Sterzel T, Kropp JP. Cities as nuclei of sustainability? Environ Plan B Urban Anal City Sci. 2017;44:425–40. https://doi.org/10.1177/0265813516638340.

[75] Amundsen H, Berglund F, Westskog H. Overcoming barriers to climate change adaptation—a question of multilevel governance? Environ Plan C Gov Policy. 2010;28:276–89. https://doi.org/10.1068/c0941.

[76] Anguelovski I, Chu E, Carmin J. Variations in approaches to urban climate adaptation: experiences and experimentation from the global south. Glob Environ Chang. 2014;27:156–67. https://doi.org/10.1016/j.gloenvcha.2014.05.010.

[77] Carmin J, Anguelovski I, Roberts D. Urban climate adaptation in the global south: planning in an emerging policy domain. J Plan Educ Res. 2012;32:18–32. https://doi.org/10.1177/0739456X11430951.

[78] Brown R. Ameliorating the effects of climate change: modifying microclimates through design. Landsc. Urban Plan. - Landsc. Urban Plan. 2011;100:372–4. https://doi.org/10.1016/j.landurbplan.2011.01.010.

[79] OECD. OECD and Bloomberg Philanthropies: cities and climate... - Google Scholar [WWW Document]. https://scholar.google.com/scholar_lookup?title=Cities%20and%20Climate%20Change%3A%20National%20Governments%20Enabling%20Local%20Action&publication_year=2014&author=OECD; 2014. [Accessed 27 April 2019].

[80] Gould SJ. Allometry and size in ontogeny and phylogeny. Biol Rev. 1966;41:587–638. https://doi.org/10.1111/j.1469-185X.1966.tb01624.x.

[81] Lee Y. An allometric analysis of the US Urban System: 1960–80. Environ Plan Econ Space. 1989;21:463–76. https://doi.org/10.1068/a210463.

[82] Schmidt-Nielsen K. Scaling: Why is animal size so important? Cambridge University Press; 1984.

[83] Small CG. The statistical theory of shape; 2012 [Springer Science & Business Media].

[84] Naroll RS, von Bertalanffy L. The principle of allometry in biology and the social sciences. Yearb: Gen. Syst; 1956.

[85] Nordbeck S. Urban allometric growth. Geogr Ann Ser B Hum Geogr. 1971;53:54–67. https://doi.org/10.2307/490887.

[86] West GB, Brown JH. The origin of allometric scaling laws in biology from genomes to ecosystems: towards a quantitative unifying theory of biological structure and organization. J Exp Biol. 2005;208:1575–92. https://doi.org/10.1242/jeb.01589.

[87] Longley PA, Batty M, Shepherd J. The size, shape and dimension of urban settlements. Trans Inst Br Geogr. 1991;16:75–94. https://doi.org/10.2307/622907.

[88] Chen Y. Characterizing growth and form of fractal cities with allometric scaling exponents [WWW document]. Discrete Dyn Nat Soc. 2010. https://doi.org/10.1155/2010/194715.

[89] Sarkar S, Phibbs P, Simpson R, Wasnik S. The scaling of income distribution in Australia: possible relationships between urban allometry, city size, and economic inequality. Environ Plan B Urban Anal City Sci. 2018;45:603–22. https://doi.org/10.1177/0265813516676488.

[90] Bettencourt LMA, Lobo J, Helbing D, Kühnert C, West GB. Growth, innovation, scaling, and the pace of life in cities. Proc Natl Acad Sci. 2007;104:7301–6. https://doi.org/10.1073/pnas.0610172104.

[91] Batty M. The size, scale, and shape of cities. Science. 2008;319:769–71. https://doi.org/10.1126/science.1151419.

[92] Bettencourt LMA. The origins of scaling in cities. Science. 2013;340:1438–41. https://doi.org/10.1126/science.1235823.

[93] Longley P, Batty M, Shepherd J, Sadler G. Do green belts change the shape of urban areas? A preliminary analysis of the settlement geography of south East England. Reg Stud. 1992;26:437–52. https://doi.org/10.1080/00343409212331347101.

[94] Bettencourt L, West G. A unified theory of urban living. Nature. 2010;467(7318):912–3.

[95] MacKenzie AR, Whyatt JD, Barnes MJ, Davies G, Hewitt CN. Urban form strongly mediates the allometric scaling of airshed pollution concentrations. Environ Res Lett. 2019;14:124078. https://doi.org/10.1088/1748-9326/ab50e3.

[96] Cottineau C, Hatna E, Arcaute E, Batty M. Diverse cities or the systematic paradox of urban scaling laws. Comput. environ. urban syst. Spatial analysis with census data: emerging issues and innovative approaches. 2017;63:80–94. https://doi.org/10.1016/j.compenvurbsys.2016.04.006.

[97] Duckworth FS, Sandberg JS. The effect of cities upon horizontal and vertical temperature gradients. Bull Am Meteorol Soc. 1954;35:198–207.

[98] Oke TR. City size and the urban heat island. Atmos Environ. 1973;1967(7):769–79. https://doi.org/10.1016/0004-6981(73)90140-6.

[99] Chandler, T.J., 1966. The climate of London. By T. J. Chandler. London (Hutchinson), 1965. Pp. 292: 86 Figures; 98 Tables; 5 Appendix Tables. £3. 10s. 0d. Q J Roy Meteorol Soc 92, 320–321. . https://doi.org/10.1002/qj.49709239230.

[100] Terjung WH, Louie SS-F. A climatic model of urban energy budgets. Geogr Anal. 1974;6:341–67. https://doi.org/10.1111/j.1538-4632.1974.tb00519.x.

[101] Eliasson I. Urban nocturnal temperatures, street geometry and land use. Atmos. Environ. Conference on the Urban Thermal Environment Studies in Tohwa. 1996;30:379–92. https://doi.org/10.1016/1352-2310(95)00033-X.

[102] Oke TR. Canyon geometry and the nocturnal urban heat island: comparison of scale model and field observations. J Climatol. 1981;1:237–54. https://doi.org/10.1002/joc.3370010304.

[103] Lee H-Y. An application of NOAA AVHRR thermal data to the study of urban heat islands. Atmospheric environ. Part B Urban Atmosphere. 1993;27:1–13. https://doi.org/10.1016/0957-1272(93)90041-4.

[104] Eagleman JR. A comparison of urban climatic modifications in three cities. Atmos Environ. 1974;1967(8):1131–42. https://doi.org/10.1016/0004-6981(74)90047-X.

[105] Oke TR, Maxwell GB. Urban heat island dynamics in Montreal and Vancouver. Atmos Environ. 1975;1967(9):191–200. https://doi.org/10.1016/0004-6981(75)90067-0.

[106] Manoli G, Fatichi S, Schläpfer M, Yu K, Crowther TW, Meili N, et al. Magnitude of urban heat islands largely explained by climate and population. Nature. 2019;573:55–60. https://doi.org/10.1038/s41586-019-1512-9.

[107] Oke TR. The energetic basis of the urban heat island. Q J Roy Meteorol Soc. 1982;108:1–24. https://doi.org/10.1002/qj.49710845502.

[108] Torok SJ, Morris JG, Skinner C, Plummer N. Urban heat island features of southeast Australian towns. Aust Met Mag. 2001;50:1–13.

[109] Zhou B, Rybski D, Kropp JP. On the statistics of urban heat island intensity. Geophys Res Lett. 2013;40:5486–91. https://doi.org/10.1002/2013GL057320.

[110] CEDA. CEDA data server, index of /badc/ukcp09/data/gridded-land-obs/gridded-land-obs-averages-5km/grid/netcdf/mean-temperature/[WWW document]. URL. . http://data.ceda.ac.uk/badc/ukcp09/data/gridded-land-obs/gridded-land-obs-averages-5km/grid/netcdf/mean-temperature/; 2011. [Accessed 2 October 2018].

[111] SolarGIS. Global solar atlas [WWW document]. URL. . https://globalsolaratlas.info/support/release-notes; 2019. [Accessed 25 January 2020].

[112] Bettencourt LMA, Lobo J, Strumsky D, West GB. Urban scaling and its deviations: revealing the structure of wealth, innovation and crime across cities. PLoS One. 2010;5:e13541. https://doi.org/10.1371/journal.pone.0013541.

[113] Office for National Statistics. Population estimates - Office for National Statistics [WWW document]. URL. https://www.ons.gov.uk/peoplepopulationandcommunity/populationandmigration/populationestimates; 2017. [Accessed 9 December 2017].

[114] Briney A. How the United Kingdom became an island nation [WWW document]. URL: ThoughtCo; 2019. https://www.thoughtco.com/geography-of-the-united-kingdom-1435710. [Accessed 4 September 2019].

[115] Kennedy J, Dunn R, McCarthy M, Titchner H, Morice C. Global and regional climate in 2016. Weather. 2017;72:219–25. https://doi.org/10.1002/wea.3042.

[116] Wan Z, Hook S, Hulley G. MOD11A1 MODIS/Terra land surface temperature/emissivity daily L3 global 1km SIN grid V006. Distributed by NASA EOSDIS Land Processes DAAC. 2015. https://doi.org/10.5067/MODIS/MOD11A1.006.Accessed 2020-05-19.

[117] Wan Z, Dozier J. A generalized split-window algorithm for retrieving land-surface temperature from space. IEEE Trans Geosci Remote Sens. 1996;34:892–905. https://doi.org/10.1109/36.508406.

[118] Wan Z. New refinements and validation of the MODIS land-surface temperature/emissivity products. Remote Sens Environ. 2008;112:59–74. https://doi.org/10.1016/j.rse.2006.06.026.

[119] Bechtel B, Sismanidis P, Voogt J, Zhan W. Seasonal surface urban Heat Island analysis, in: 2019 joint urban remote sensing event (JURSE). Presented at the 2019 joint urban remote sensing event (JURSE); 2019. p. 1–4. https://doi.org/10.1109/JURSE.2019.8808982.
[120] Whitehand JWR, Whitehand SMR. The physical fabric of town centres: the agents of change. Trans Inst Br Geogr. 1984;9:231. https://doi.org/10.2307/622170.
[121] Arnfield AJ, Grimmond CSB. An urban canyon energy budget model and its application to urban storage heat flux modeling. Energ Buildings. 1998;27:61–8. https://doi.org/10.1016/S0378-7788(97)00026-1.
[122] Nunez M, Oke TR. The energy balance of an urban canyon. J Appl Meteorol. 1977;16:11–9. https://doi.org/10.1175/1520-0450(1977)016<0011:TEBOAU>2.0.CO;2.
[123] Clinton N, Gong P. MODIS detected surface urban heat islands and sinks: global locations and controls. Remote Sens Environ. 2013;134:294–304. https://doi.org/10.1016/j.rse.2013.03.008.
[124] Schwarz N, Manceur AM. Analyzing the influence of urban forms on surface urban heat islands in Europe. J Urban Plan Dev. 2014;141(3):A4014003.
[125] Fuller RA, Gaston KJ. The scaling of green space coverage in European cities. Biol Lett. 2009;5:352–5. https://doi.org/10.1098/rsbl.2009.0010.
[126] Hoornweg D, Sugar Lorraine, Gómez Claudia Lorena Trejos. Cities and greenhouse gas emissions: moving forward. Environ Urban. 2011;23:207–27. https://doi.org/10.1177/0956247810392270.
[127] Li R, Dong L, Zhang J, Wang X, Wang W-X, Di Z, et al. Simple spatial scaling rules behind complex cities. Nat Commun. 2017;8:1841. https://doi.org/10.1038/s41467-017-01882-w.
[128] Yow DM. Urban heat islands: observations, impacts, and adaptation. Geogr Compass. 2007;1:1227–51. https://doi.org/10.1111/j.1749-8198.2007.00063.x.
[129] Zhou B, Lauwaet D, Hooyberghs H, De Ridder K, Kropp J, Rybski D. Assessing seasonality in the surface urban heat island of London. J Appl Meteorol Climatol. 2016;55:493–505. https://doi.org/10.1175/JAMC-D-15-0041.1.
[130] Zhao L, Lee X, Smith RB, Oleson K. Strong contributions of local background climate to urban heat islands. Nature. 2014;511:216–9. https://doi.org/10.1038/nature13462.

Data sources

[131] Meridian_data. https://digimap.edina.ac.uk/webhelp/os/data_information/os_products/meridian_2.htm; 2017. data downloaded on 31st January 2017.
[132] MODIS/terra land surface temperature and emissivity daily L3 global 1km Grid SIN V006. https://search.earthdata.nasa.gov/search. Data downloaded on 23rd August 2017c(Earthdata, 2017). For a description of the dataset, see . https://lpdaac.usgs.gov/products/mod11a1v006/.
[133] . https://www.planninghelp.cpre.org.uk/planning-explained/history-of-the-planning-system. [Accessed 26 September 2019]